Journal of Solid State Chemistry 183 (2010) 2116–2120

Contents lists available at ScienceDirect

Journal of Solid State Chemistry

journal homepage: www.elsevier.com/locate/jssc

Facile synthesis of mesophase pitch/exfoliated graphite nanoplatelets nanocomposite and its application as anode materials for lithium-ion batteries

Yi-Shuang Yang, Cheng-Yang Wang*, Ming-Ming Chen, Zhi-Qiang Shi, Jia-Ming Zheng

Key Laboratory for Green Chemical Technology of Ministry of Education, School of Chemical Engineering and Technology, Tianjin University, Tianjin 300072, PR China

ARTICLE INFO

Article history:
Received 21 February 2010
Received in revised form
24 May 2010
Accepted 12 July 2010
Available online 15 July 2010

Keywords:
Mesophase pitch
Exfoliated graphite nanoplatelets
Nanocomposite
Anode material
Lithium-ion batteries

ABSTRACT

Mesophase pitch (MP)/exfoliated graphite nanoplatelets (GNPs) nanocomposite has been prepared by an efficient method with an initiation of graphite intercalation compounds (GIC). X-ray diffraction, optical microscopy, high-resolution transmission electron microscopy and scanning electron microscopy analysis techniques are used to characterize the samples. It is observed that GIC has exfoliated completely into GNPs during the formation of MP/GNPs nanocomposite and the GNPs are distributed uniformly in MP matrix, which represent a conductive path for a movement of electrons throughout the composites. Electrochemical tests demonstrate that the carbonized MP/GNPs nanocomposite displays higher capacity and better cycle performance in comparison with the pure carbonized MP. It is concluded that such a large improvement of electrochemical performance within the nanocomposite may in general be related to the enhanced electronic conductivity, which is achieved by good dispersion of GNPs within MP matrix and formation of a 3D network of GNPs.

1. Introduction

As one of the most advanced power sources, lithium-ion batteries (LIB) have attracted special attention in the scientific and industrial fields due to their high electromotive force and high energy density [1]. For an anode material in LIB, graphitic materials are extensively spread as commercial anode materials in LIB due to their flat potential profile versus lithium and structural stability during cycling [2,3]. However, graphite suffers from a relatively small capacity. Thus, in order to meet the increasing demand for batteries with higher energy density, further researches have been made to explore new electrode materials for overcoming the limited capacity of graphite [1,4]. Among the carbonaceous materials, disordered carbons, obtained at temperatures lower than 1000 °C, could be one of the promising alternatives as an anode in LIB because of their cheap production, high specific capacity and wide redox potential range compared to conventional graphite carbon anode electrodes [5–7]. However, these advantages are accompanied by undesirable irreversible capacities and poor cycling performances due to their lower electronic conductivity.

In order to improve the cycling stability and enhance the reversible capacities of the disordered carbons anode, it is important to achieve high material electronic conductivity both intrinsically and extrinsically [8]. The extrinsic electronic conductivity can be easily achieved by mixing the electrode material with conducting additives such as nano-sized acetylene black [9]. While for intrinsic electronic conductivity, designing and synthesizing nanocomposites with conductive fillers finely dispersed in a carbon matrix have been proved to be an effective approach [10].

Among the various known conductive fillers, exfoliated graphite nanoplatelets (GNPs) were very promising and thus were selected as the filler in the present study, because of their nanometer-scale dimensions, high electronic conductivity, high mechanical strength; Besides, functional groups, such as C–O–C, C–OH and C–O existing on the surface of graphite nanoplatelets, can promote a good affinity of the GNPs to both the organic compounds and the polymer [11–13]. However, uniform dispersion of GNPs in polymer matrices is still difficult for their strong intrinsic van der Waals attraction between sheets (over 2 eV nm^{-2} [14]), high aspect ratio and high surface area.

In this study, we reported an efficient method to synthesize uniform mesophase pitch (MP)/GNPs nanocomposite utilizing graphite intercalation compounds (GIC) as an initiator, which was attributed to the well-uniform dispersion of the GIC in MP. Additionally, the GIC was exfoliated into GNPs during the preparation of MP/GNPs nanocomposite and the GNPs were distributed uniformly in MP matrix, simplifying the thermal shock exfoliation process and reducing cost. The electrochemical performance of the carbonized MP/GNPs nanocomposite was

* Corresponding author. Fax: +86 22 27890481.
E-mail address: cywang@tju.edu.cn (C.-Y. Wang).

0022-4596/$ - see front matter Crown Copyright © 2010 Published by Elsevier Inc. All rights reserved.
doi:10.1016/j.jssc.2010.07.011

investigated, on the basis of the morphology and structure, by a variety of electrochemical testing techniques. Compared with the carbonized (unmodified) MP anode, the carbonized MP/GNPs nanocomposite shows clear advantages in electrochemical behaviors in terms of high reversible capacity and relatively stable cycle performance.

2. Experimental

2.1. Materials and synthesis

In this research, a kind of isotropic petroleum pitch was used as the precursor of MP. The GIC used in the present study was prepared from natural graphite flake through intercalation and chemical oxidation in the presence of concentrated H_2SO_4 and HNO_3. It is composed of layered and compact nanoplatelets of graphite shown in Fig. 1. Prior to preparation of the composites, the petroleum pitch was proportionally well-mixed with GIC powders and the GIC content in raw pitch was 0% and 7% in weight. Then the mixtures were added into a stainless-steel reactor and kept at 420 °C for 10 h to provide the formation of uniform composites. During the heat treatment, an agitation of 70 rpm was maintained and a nitrogen flow of 0.5 $m^3\ h^{-1}$ was applied to remove volatile compounds. The resulting samples continued to be carbonized at 700 °C under protection of nitrogen and were named as CMP and CMP/GNPs nanocomposite, respectively.

2.2. Sample characterization

The dispersed state of graphite nanoplatelets in MP matrix was characterized by the optical microscopy (OM, Nikon E600 POL). The structure and morphology of the MP/GNPs nanocomposite were analysed by high-resolution transmission electron microscopy (HRTEM, TECNAI G^2 F20, 200 kV, FEI, Netherlands) and scanning electron microscopy (SEM, Philips XL30). X-ray diffraction (XRD) analysis was conducted on a D/Max2500 X-ray diffractometer using Cu$K\alpha$ radiation (40 kV, 200 mA, $\lambda = 1.54056$ Å).

2.3. Cell preparation and electrochemical tests

Two-electrode batteries were prepared with polyethylene membrane as separator. Reference and counter electrodes were lithium sheets and the working electrode consisted of a mixture of active materials and poly (vinyl difluoride) (PVDF) at a weight ratio of 92:8. The electrolyte used was 1 M $LiPF_6$, dissolved in 1/1/1(volume) ethylene carbonate (EC)/dimethyl carbonate (DMC)/ethyl methyl carbonate (EMC). Coin cells were assembled in a high purity argon-filled glove box. The galvanostatic charge-discharge experiment was carried out on a Land CT2001A battery test instrument at a constant current density of 80 mA g^{-1} between cut-off potentials of 0.01 and 2.5 V.

3. Results and discussion

3.1. Characterization of the nanocomposite

Typical OM images of MP and MP/GNPs nanocomposite are presented in Fig. 2. Fig. 2(a) shows that MP without addition of GIC exhibits large anisotropic domain, while in Fig. 2(b), MP/GNPs nanocomposite exhibits smaller anisotropic domain. This is because the graphite nanoplatelets prevent the coalescence of the mesophase domains during heat treatment. White plate phase corresponds to GNPs in MP matrix. According to OM observations of the MP/GNPs nanocomposite, GIC has exfoliated completely into GNPs and the GNPs are distributed uniformly in MP matrix, allowing the formation of numerous contacts between different GNPs particles.

The fractured morphology and nanostructure of MP/GNPs nanocomposite were characterized by SEM and TEM observations. Fig. 3(a) shows fractured morphology of MP/GNPs nanocomposite

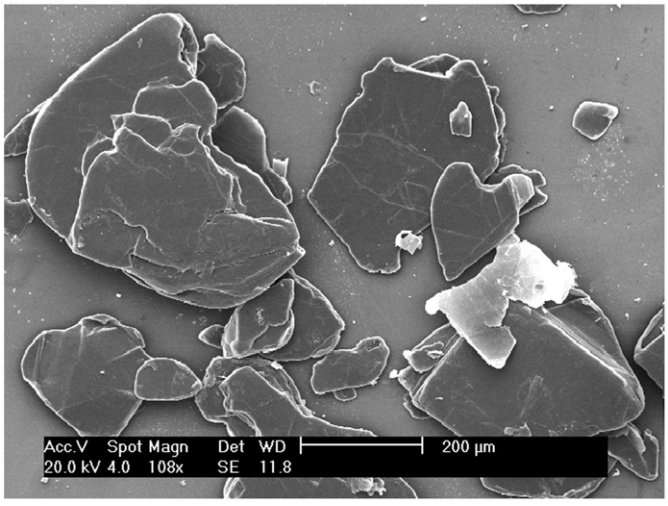

Fig. 1. SEM image of GIC.

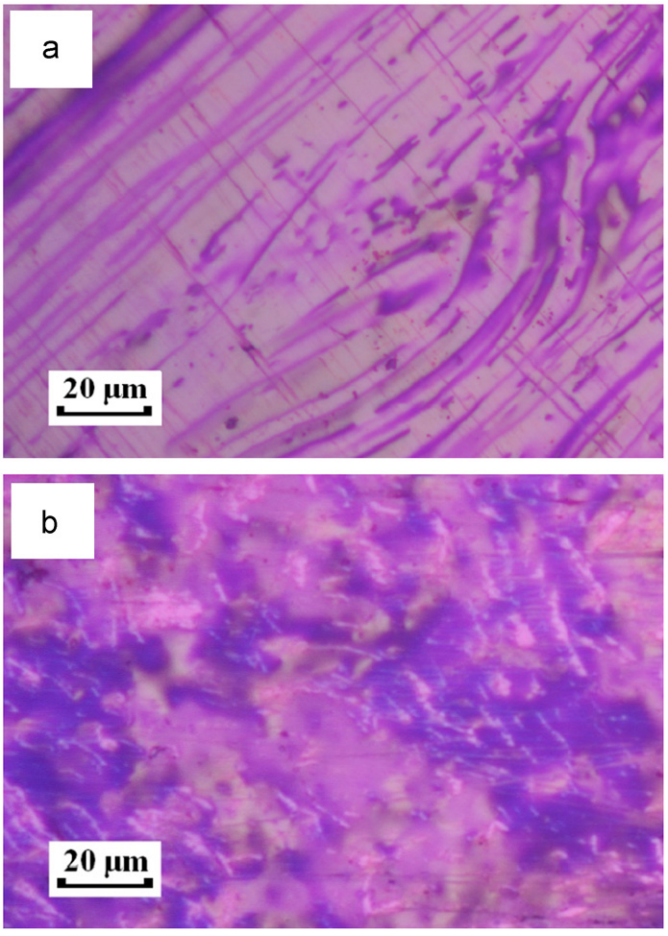

Fig. 2. OM images of (a) MP and (b) MP/GNPs nanocomposite.

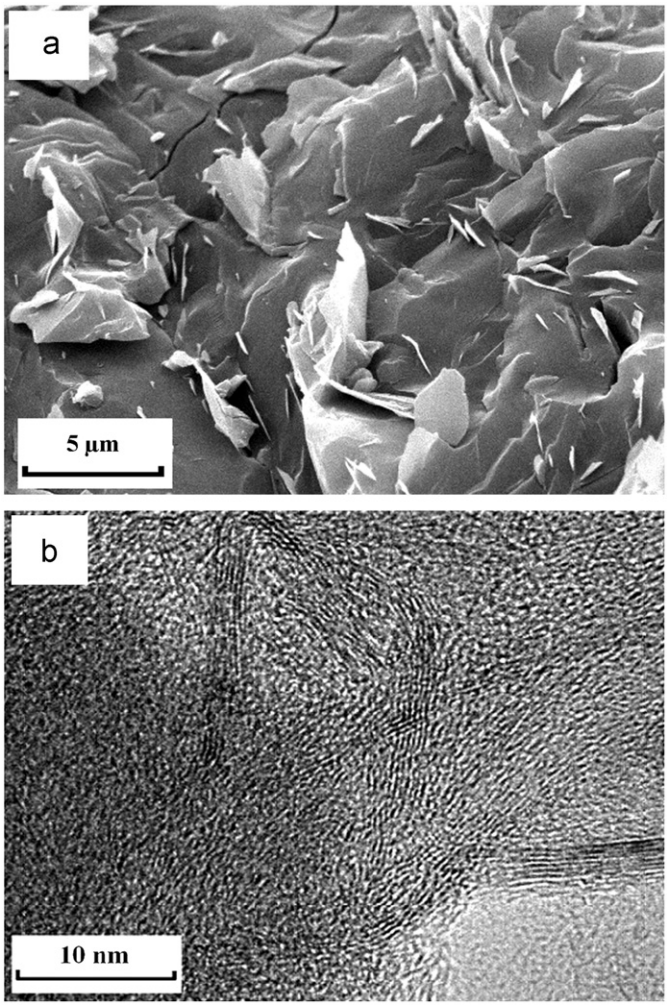

Fig. 3. (a) SEM image of fractured cross-section of MP/GNPs nanocomposite. (b) TEM image of MP/GNPs nanocomposite.

at a magnification of 4000. As one can see, infinite cluster of graphite nanoplatelets is formed in MP matrix, which penetrates throughout the sample and represents a conductive path for a movement of electrons throughout the composites. The SEM image of MP/GNPs nanocomposite reveals that after polymerization, GIC has exfoliated into the form of nanoplatelets and the graphite nanoplatelets are well-dispersed in MP matrix. Fig. 3(b) shows a typical HRTEM cross-sectional image of MP/GNPs nanocomposite. The HRTEM image shows the interface between the MP and GNPs. The curly and parallel lines represent the cross-sections of the GNPs, while the amorphous structure image is MP. The results further confirm the uniform distribution of GNPs in MP matrix and the formation of a 3D network of GNPs.

The XRD patterns of CMP, CMP/GNPs, GNPs and GIC are shown in Fig. 4. For the CMP and GNPs, the (0 0 2) diffraction peaks appear at 25.4° and 26.4°, respectively. As shown as Fig. 4(d), the GIC exhibits a sharp diffraction peak at 26.0° with an interlayer spacing of 0.3422 nm, corresponding to the layered structure of the GIC. In the XRD pattern of CMP/GNPs nanocomposite (see Fig. 4(b)), the sharp GIC peak disappears, but an additional peak appears at 26.4°, which attributed to the (0 0 2) diffraction peak of the GNPs. The XRD results clearly demonstrate that GIC was fully exfoliated into GNPs and the GNPs were incorporated into the MP matrix. The regular and periodic structure of GIC disappeared.

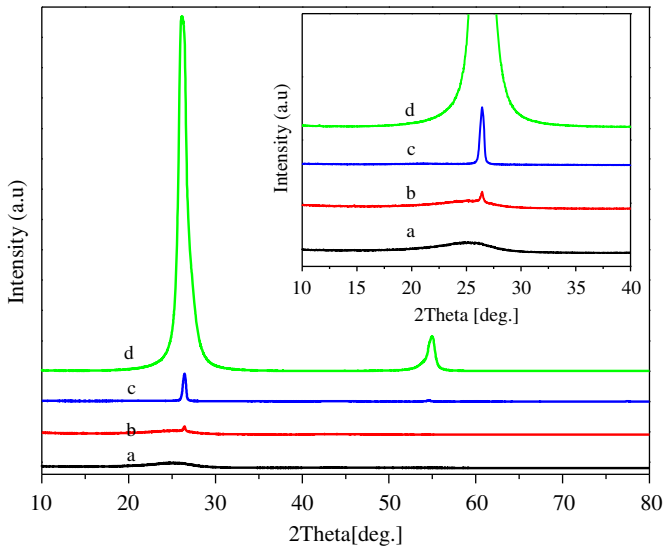

Fig. 4. XRD patterns of samples: (a) CMP, (b) CMP/GNPs, (c) GNPs and (d) GIC.

3.2. Electrochemical tests

As the GNPs used in our experiments have very high electronic conductivity, the successful introduction of GNPs into MP matrix may enhance the electronic conductivities of the intra- and inter-MP particles, which is favorable for use of MP as an anode material for LIB.

To demonstrate the potential application of the present CMP/GNPs nanocomposite with enhanced electronic conductivity, we carried out a preliminary investigation into its electrochemical performance toward the lithium insertion/extraction compared with that of CMP. It was found that the first discharge/charge voltage profiles (see Fig. 5(a)) for CMP and CMP/GNPs nanocomposite are very similar, implying that the addition of GNPs to CMP does not change the electrochemical performance of the CMP. In the first discharge curve, there exist two sloping voltage ranges (1.20–0.80 and 0.80–0.01 V versus Li^+/Li) that can be discerned in the composite sample. The first slope is related with irreversible reactions on the carbon particles surface and the formation of the solid electrolyte inter-phase (SEI) film, while the potential slope in 0.80–0.01 V corresponds to the insertion of lithium ions into the CMP/GNPs nanocomposite anode [15]. The initial charge capacity of CMP/GNPs nanocomposite anode is 381.2 mAh g^{-1}, which is larger than the theoretical capacity for graphite (372 mAh g^{-1} for LiC_6 composition), although the polarization between the discharging and charging performances. Generally, carbon materials, prepared at low-temperature (500–1000 °C), show a large hysteresis in the voltage curves, which is mainly related to lithium doping at the inner surface of the cavities constructed by the edges of disordered staking of crystallites [16–18]. However, a relatively lower voltage hysteresis is observed on the voltage profile of CMP/GNPs nanocomposite, which is appropriate to the practical application. It is also worth noting that the initial Coulombic efficiency of CMP/GNPs nanocomposite is 57.3%, which is much larger than that of CMP (48.2%). In the subsequent cycles, the Coulombic efficiency of CMP/GNPs nanocomposite increases to nearly 93% for the 2nd cycle, 98.5% for the 25th cycle and 98.8% for the 50th cycle, indicating that the newly formed SEI film and the CMP/GNPs nanocomposite electrode are stable during cycling.

Another excellent property of the CMP/GNPs nanocomposite is the significantly enhanced cycling performance and specific capacity compared with the pure CMP and the commercial MCMB

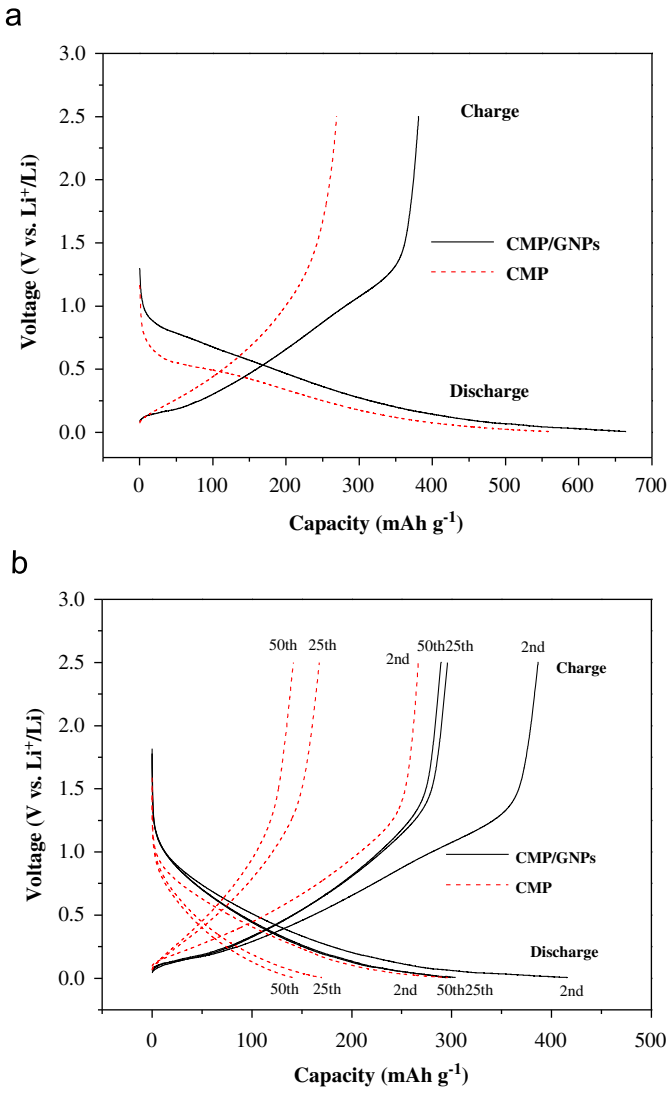

Fig. 5. (a) First and (b) 2nd, 25th and 50th discharge/charge voltage profiles of CMP and CMP/GNPs nanocomposite cycled at a constant current density of 80 mA g^{-1}.

(heat treatment at 2800 °C, Tie Cheng Co., Ltd.). The results are shown in Fig. 6, in which a current density of 80 mA g^{-1} has been employed. The contribution to the capacity from GNPs is nearly negligible, because the GNPs content in the composite is only 7 wt% and the capacity of GNPs itself is very small [19]. However, the specific capacity of the CMP/GNPs nanocomposite was still calculated on the basis of the whole mass. It is exciting to note that the CMP/GNPs nanocomposite is better than the commercial MCMB in terms of reversible capacity. It can also be observed that the first charge capacity of CMP is 269.3 mAh g^{-1}. However, this value quickly decreases to 167.6 mAh g^{-1} after 25 cycles, and 130.6 mAh g^{-1} after 50 cycles, indicating poor capacity retention. On the other hand, MP/GNPs nanocomposite exhibits an initial charge capacity of 381.2 mAh g^{-1}. Furthermore, its cycling performance is drastically enhanced, as seen in the figure. After 50 cycles, the charge capacity still remained at 289.5 mAh g^{-1}, which is about 75.9% retention of the initial reversible capacity. The results indicate that introducing GNPs into CMP matrix is an effective way to improve the cycling performance of the composite material. Such an improvement can be attributed to the uniform distribution of GNPs particles and the formation of a 3D network of GNPs within CMP matrix, thus enhancing the

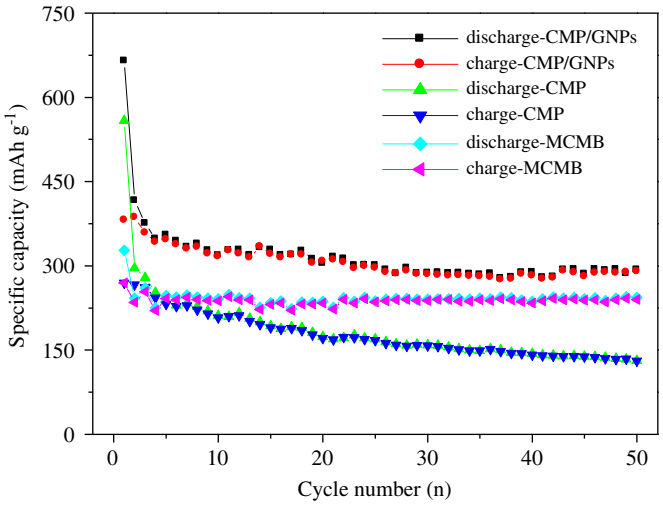

Fig. 6. Cycle performances of CMP, CMP/GNPs nanocomposite and a commercial MCMB at a constant current density of 80 mA g^{-1}.

electronic conductive. The 3D network of GNPs can be considered as a 3D current collector network, which provided negligible times of the electronic carriers to the Li^+ contact (electrolyte) and thus to minimize solid state diffusion length for Li [10,20].

4. Conclusions

In summary, we have developed an effective strategy to fabricate MP/GNPs nanocomposite with the initiation of GIC, in which the GIC had exfoliated completely into GNPs during the formation of MP/GNPs nanocomposite and the GNPs were distributed uniformly in MP matrix. The CMP/GNPs nanocomposite electrode showed better electrochemical performance than the pure CMP in regard to specific capacity and cycling capability. The improvement of electrochemical performance can be attributed to the as-formed 3D network of GNPs and the enhanced electric conductivity. The 3D network of GNPs can act as a 3D current collector network and help to bring the electronic carriers as rapidly as possible from the current collector to the Li^+ contact (electrolyte), thus to minimize solid state diffusion length for Li.

Acknowledgments

This work was supported by the National Natural Science Foundation of China (50902102), and Tianjin Application Bases and Advanced Technology Research Program Key Projects (08JCZDJC17000).

References

[1] S.M. Paek, E. Yoo, I. Honma, Nano Lett. 9 (2009) 72–75.
[2] A. Concheso, R. Santamaría, R. Menéndez, J.M. Jiménez-Mateos, R. Alcántara, P. Lavela, J.L. Tirado, Carbon 44 (2006) 1762–1772.
[3] E. Markevich, E. Pollak, G. Salitra, D. Aurbach, J. Power Sources 174 (2007) 1263–1269.
[4] P. Guo, H.H. Song, X.H. Chen, Electrochem. Commun. 11 (2009) 1320–1324.
[5] N. Ogihara, Y. Igarashi, A. Kamakura, K. Naoi, Y. Kusachi, K. Utsugi, Electrochim. Acta 52 (2006) 1713–1720.
[6] F. Bonino, S. Brutti, P. Reale, B. Scrosati, L. Gherghel, J. Wu, K. Miillen, Adv. Mater. 17 (2005) 743–746.
[7] I. Watanabe, T. Doi, J.I. Yamaki, Y.Y. Lin, G.Ting-Kuo Fey, J. Power Sources 176 (2008) 347–352.
[8] J.C. Badot, É. Ligneel, O. Dubrunfaut, D. Guyomard, B. Lestriez, Adv. Funct. Mater. 19 (2009) 2749–2758.
[9] H.Y. Wang, T. Umeno, K. Mizuma, M. Yoshio, J. Power Sources 175 (2008) 886–890.

[10] Z.H. Wen, Q. Wang, Q. Zhang, J.H. Li, Adv. Funct. Mater. 17 (2007) 2772–2778.
[11] S. Kim, I. Do, L.T. Drzal, Macromol. Mater. Eng. 294 (2009) 196–205.
[12] F. He, S. Lau, H.L. Chan, J.T. Fan, Adv. Mater. 21 (2009) 710–715.
[13] M. Green, G. Marom, J. Li, J.K. Kim, Macromol. Rapid Commun. 29 (2008) 1254–1258.
[14] R. Zacharia, H. Ulbricht, T. Herte, Phys. Rev. B 69 (2004) 155406 (7pp).
[15] L.W. Ji, X.W. Zhang, Nanotechnology 20 (2009) 155705 (7 pp).
[16] Z.H. Yi, X.Y. Han, C.C. Ai, Y.G. Liang, J.T. Sun, J. Solid State Electrochem. 12 (2008) 1061–1066.
[17] M. Winter, J.Q. Besenhard, M.E. Spahr, P. Novak, Adv. Mater. 10 (1998) 725–763.
[18] H.S. Zhou, S.M. Zhu, M. Hibino, I. Honma, M. Ichihara, Adv. Mater. 15 (2003) 2107–2111.
[19] J. Makovička, M. Sedlaříková, A. Arenillas, J. Velická, J. Vondrák, J. Solid State Electrochem. 13 (2009) 1467–1471.
[20] N.A. Kaskhedikar, J. Maier, Adv. Mater. 21 (2009) 2664–2680.